



HAL
open science

Preparation of miniaturized hydrophilic affinity monoliths: Towards a reduction of non-specific interactions and an increased target protein density

Julie GIL, Isabelle Krimm, Vincent Dugas, Claire Demesmay

► To cite this version:

Julie GIL, Isabelle Krimm, Vincent Dugas, Claire Demesmay. Preparation of miniaturized hydrophilic affinity monoliths: Towards a reduction of non-specific interactions and an increased target protein density. *Journal of Chromatography A*, 2023, 1687, pp.463670. 10.1016/j.chroma.2022.463670 . hal-03888930

HAL Id: hal-03888930

<https://hal.science/hal-03888930v1>

Submitted on 7 Dec 2022

HAL is a multi-disciplinary open access archive for the deposit and dissemination of scientific research documents, whether they are published or not. The documents may come from teaching and research institutions in France or abroad, or from public or private research centers.

L'archive ouverte pluridisciplinaire **HAL**, est destinée au dépôt et à la diffusion de documents scientifiques de niveau recherche, publiés ou non, émanant des établissements d'enseignement et de recherche français ou étrangers, des laboratoires publics ou privés.

1 Preparation of miniaturized hydrophilic affinity monoliths: towards a
2 reduction of non-specific interactions and an increased target protein
3 density

4
5 Julie GIL¹, Isabelle Krimm², Vincent Dugas¹, Claire Demesmay¹

6
7
8 *1 – Université de Lyon, CNRS, Université Claude Bernard Lyon 1, Institut des Sciences Analytiques, UMR 5280, 5*
9 *rue de la Doua, F-69100 VILLEURBANNE, France*

10 *2 – Université de Lyon, Université Claude Bernard Lyon 1, INSERM 1052, CNRS 5286, Centre Léon Bérard, Centre*
11 *de recherche en cancérologie de Lyon, Small Molecules for Biological Targets Team, Lyon, 69373, France*

12

13

14

15

16

17

18 Keywords

19 Frontal affinity chromatography, hydrophilic organic monolith, non-specific interactions, fragment
20 screening

21

22

23 Abstract

24 In affinity chromatography, non-specific interactions between the ligands and the affinity column may
25 affect the results, leading to misinterpretations during the investigation of protein-ligand interactions
26 (detection of false positives in ligand screening, lack of specificity in purification). Such non-specific
27 interactions may arise both from the underlying support or from the target protein itself. If the second
28 ones are protein-dependent (and cannot be studied in a general framework), the first ones occur in
29 the same way regardless of the immobilized target. We propose a methodology to identify the origin
30 of such non-specific interactions with the underlying material of the affinity column. This methodology
31 relies on the systematic investigation of the retention behavior of a set of 41 low-molecular weight
32 compounds covering a wide chemical space (net charge, log D, functionality). We first demonstrate
33 that the main source of non-specific interactions on the most commonly used GMA-co-EDMA monolith
34 comes from hydrophobic effects. To reduce such non-specific interactions, we developed a new
35 hydrophilic glycidyl methacrylate-based monolith by replacing the EDMA crosslinker by the more
36 hydrophilic N-N' Methylenebisacrylamide (MBA). Optimization of the synthesis parameters (monomer
37 content, initiation type, temperature) has focused on the reduction of non-specific interaction with
38 the monolithic support while maximizing the amount of protein that can be grafted onto the monolith
39 at the issue of its synthesis. The retention data of the 41 test solutes on the new poly(GMA-co-MBA)
40 monolith shows a drastic reduction of non-specific interactions except for cationic compounds. The
41 particular behavior of cationic compounds is due to their electrostatic interactions with carboxylic
42 groups resulting from the partial acidic hydrolysis of amide groups of MBA during the epoxide ring
43 opening step. So, the ring opening step in acidic media was replaced by a hot water treatment to avoid
44 side reaction on MBA. The new monolith poly(GMA-co-MBA) not only has improved hydrophilic
45 surface properties but also a higher protein density ($16 \pm 0.8 \text{ pmol cm}^{-1}$ instead of $8 \pm 0.3 \text{ pmol cm}^{-1}$).
46 To highlight the benefits of this new hydrophilic monolith for affinity chromatographic studies, frontal
47 affinity chromatography experiments were conducted on these monoliths grafted with con A.

48

49 1- Introduction

50 Affinity monolith chromatography (AMC) is a type of liquid chromatography that uses monolithic
51 supports functionalized with biological targets such as proteins, receptors, antibodies or enzymes [1–
52 3]. AMC is a powerful method for clean-up and preconcentration purposes in sample treatment [4,5],
53 chiral separation [6] and ligand or fragment screening in Drug discovery [7,8]. Applications also include
54 the study of biological interactions to get information on the stoichiometry, thermodynamics and
55 kinetics of the interaction between the immobilized biological target and ligands in solution.

56 Miniaturized affinity monolith chromatography μ AMC, with columns in the few tens μ m range covers
57 all the application fields of AMC with the tremendous advantage of reducing the quantity of biological
58 material to be immobilized.

59 Several reasons have driven the development of miniaturized affinity chromatography with monolithic
60 supports. First, these supports are synthesized *in-situ* as continuous bed supports avoiding the
61 cumbersome filling of columns with particles. Their external porosity can be tuned to increase their
62 permeability and decrease back pressures thus allowing higher flow rates (useful for increasing the
63 throughput in screening campaigns, for decreasing the percolation time in purification or clean up
64 applications). Whatever the application field, the underlying monolithic material supporting the
65 biomolecules must satisfy two main criteria: the quantity of protein per unit volume must be as high
66 as possible and its intrinsic capacity to limit non-specific interactions. The quest for a stealthy
67 underlying support in affinity chromatography is a complex and difficult task [9,10].

68 Organic monoliths are usually preferred to their silica counterparts for their easier preparation
69 (thermally or photochemically initiated polymerization). Moreover the great diversity of
70 commercially available monomers allows tuning their surface properties and adjusting available
71 functional moieties for their subsequent grafting with a biological target [11]. They also usually offer a
72 satisfactory mechanical resistance and a tunable permeability allowing their *in-line* coupling with
73 another separation dimension (liquid chromatography or capillary electrophoresis) [12–14]. A great
74 diversity of organic monoliths has been synthesized. Among those, GMA-co-EDMA monoliths have
75 found applications in many areas (for the preparation of IMERS dedicated to *on-line* solid-supported
76 enzymatic digestion, immunoaffinity preconcentration, separation...)[12,15–17]. Moreover, their
77 synthesis is well-documented, they present a satisfactory chemical and thermal stability, and their
78 surface epoxy groups open multiple grafting-ways to prepare a wide range of stationary phases, from
79 ion-exchange to affinity columns through biomolecules immobilization (*e.g.*, aptamers and proteins).

80 Despite their frequent use, there is very little information on the non-specific interactions generated
81 by these GMA-co-EDMA monolithic based stationary phases. During a previous ligand/protein
82 interaction study by AMC [7], we have noticed that non-specific interactions can be non negligible
83 when these GMA-co-EDMA monoliths are used as underlying material for affinity columns. Indeed,
84 GMA-co-EDMA monoliths are used in experimental conditions close to physiological conditions (purely
85 aqueous medium at pH 7.4, with high salt concentration) favoring secondary interactions by
86 hydrophobic effect. We have shown that such non-specific interactions occur regardless of the mode
87 of grafting but are of less importance after grafting according to the Schiff base method *i.e.*, when
88 residual reduced aldehyde groups remain at the monolith surface instead of epoxy ones even after

89 end-capping. The existence of such interactions can lead to (i) a lack of specificity/recovery if they are
90 used for purification/preconcentration, (ii) a lack of recovery of the products resulting from the
91 enzymatic digestion (for IMERS), (iii) the detection of false positives in the case of ligand screening and
92 to (iv) a misestimation of thermodynamics parameters such as affinity constant determination.
93 Because non-specific interactions are a concern in bioaffinity chromatography, their characterization
94 seems a prerequisite to any stationary phase optimization. To our knowledge, sources of non-specific
95 interactions with the underlying support on affinity monoliths have not been thoroughly investigated.
96 For instance, no dedicated method was developed and accepted to characterize the level and origin of
97 non-specific interactions of small molecules on monolithic phases used as chromatographic underlying
98 support for affinity columns.

99 Our study stems on improving the conditions for detecting low affinities in affinity chromatography by
100 reducing unwanted interactions with the chromatographic support. In a preliminary investigative
101 study, we report a methodology aiming at characterizing non-specific interactions due to the- GMA-
102 co-EDMA underlying material widely used for the preparation of affinity columns. To achieve this task,
103 we selected a set of 41 molecules from a library of fragment-like molecules covering the whole range
104 of physico-chemical properties in terms of net charge, logD, H-bond donor and acceptor. The physical-
105 chemical properties and chemical structures of the set of fragments are detailed in Table S1. Based on
106 the outcomes of the preliminary study (non-specific interactions mainly due to hydrophobic effects),
107 we propose the synthesis of a new glycidyl based monolith, by using MBA crosslinker (instead of EDMA)
108 to increase the hydrophilicity of the resulting monolith. Both the grafting capacity and the surface
109 properties regarding the non-specific interactions of the newly prepared monolith are optimized and
110 characterized. Non-specific interactions are characterized using the developed methodology based on
111 the library of small chemical compounds. The grafting capacity is evaluated by determining the amount
112 of biological active sites present at the monolith surface after the grafting of a biological target onto
113 the monolith (amount of sites able to bind a ligand of known activity). Streptavidin is used as model
114 target protein and HABA as a test ligand. Finally, to evaluate the improvement of the new monolith in
115 affinity chromatography, low affinity ligands are used on a Concanavalin A grafted monolith. These
116 experiments highlight the benefits associated with reduced non-specific interactions and an increased
117 target protein density. All these experiments are carried out by frontal affinity experiments (with a
118 dedicated in-house developed instrumentation [18]) as described in the Material and Methods
119 Section.

120

121

122 2- Material and methods

123 2.1- Reagents and Buffers.

124 Streptavidin (from *Streptomyces avidinii*, affinity purified, ≥ 13 U mg^{-1} of protein), Concanavalin A (Con
125 A) from *Canavalia ensiformis*, (3-methacryloxypropyl)-trimethoxysilane (γ -MAPS), ethylene
126 dimethacrylate (EDMA), glycidyl methacrylate (GMA), acrylamide, N,N'-Methylenebis(acrylamide)
127 (MBA), Acrylamide (AA), 1- propanol, 1,4-butanediol, dimethyl sulfoxide (DMSO), sodium periodate,
128 lithium hydroxide, dipotassium hydrogen phosphate (K_2HPO_4), o-phosphoric acid, sulfuric acid, sodium
129 cyanoborohydride, triethylamine (TEA), azobis(isobutyronitrile) (AIBN), 4'-Hydroxyazobenzene-2-
130 carboxylic acid (HABA), p-nitrophenyl- α -D-mannopyranoside (α PNM), p-nitrophenyl- α -D-
131 glucopyranoside (α PNG) and p-nitrophenyl- α -D-galactopyranoside (α PNGal) and ligands (Table S1)
132 were purchased from Sigma-Aldrich (L'Isle d'Abeau Chesne, France). All aqueous solutions were
133 prepared using >18 M Ω deionized water. Phosphate buffer was prepared by dissolving 1.17 g of K_2HPO_4
134 in 100 mL of ultrapure water and the pH was adjusted to 7.4 with phosphoric acid.

135 2.2- Monolithic capillary column synthesis

136 Fused-silica capillaries with UV transparent coating (TSH, 75- μm i. d.) or polyimide coating (TSP, 75- μm
137 i.d.) were purchased from Polymicro Technologies (Molex). In all cases, capillaries were pre-treated by
138 flushing capillaries with a 5% (v/v) solution of γ -MAPS in methanol/water (95/5, v/v) with 2.5% TEA for
139 1 h at 7 bar. Next, they were rinsed with methanol for 15 min at 7 bar and dried at room temperature
140 under nitrogen stream.

141 2.2.1 GMA-co-EDMA Monolith synthesis:

142 Poly(GMA-co-EDMA) monoliths were synthesized as described in a previous work [7]. The
143 polymerization mixture was prepared by mixing 0.9 mL GMA, 0.3 mL EDMA, 1.05 mL 1-propanol, 0.6
144 mL 1,4-butanediol, 0.15 mL ultra-pure water and 12 mg of AIBN initiator. The pre-treated capillary (TSH
145 Capillary) was then filled with the polymerization mixture under 1 bar N_2 pressure. The
146 photopolymerization reaction was performed in a Bio-link UV cross-linker (VWR International, France)
147 under 365 nm UV light for a total energy of 6 J cm^{-2} . To localize the monolith inside the silica capillary,
148 a PEEK tubing (380 μm i. d.) was used as a mask to cover non-irradiated areas. After polymerization,
149 the capillary was rinsed with methanol for 1 h.

150 2.2.2 GMA-co-MBA monolith synthesis

151 Poly(GMA-co-MBA) monoliths were prepared as follows, adapting protocols from [19]. First, a mixture
152 of solvents was prepared by mixing 3330 mg of DMSO, 1480 mg of 1,4-butanediol and 1850 mg of

153 dodecanol. Then, 320 mg of MBA were added and sonicated 1 h at room temperature. After the
154 dissolution of MBA, 480 mg of GMA were added and sonicated 1 h at room temperature. 8 mg of AIBN
155 were added and the final mixture was sonicated 15 min at room temperature. The pre-treated capillary
156 (TSP Capillary) was then filled with the polymerization mixture under 1 bar N₂ pressure and the ends
157 of the capillary sealed. The polymerization reaction was performed in water bath at 57°C for 18 hours.
158 After polymerization monoliths were rinsed with methanol for 1 h.

159 2.3 Protein (streptavidin) immobilization

160 Streptavidin was grafted using the Schiff base method as previously described [7]. First, the epoxy
161 groups of the GMA-co-EDMA monoliths were hydrolyzed into diols flowing 1 M sulfuric acid for 2 h at
162 7 bar. After water rinsing, the diol-monolith was oxidized to aldehyde using a 0.12 M NaIO₄ solution at
163 pH 5.5. Then, a 1 mg mL⁻¹ Streptavidin and 4 mg mL⁻¹ NaBH₃CN solution in 67 mM phosphate buffer
164 (pH 6) was percolated through the column for 18 h at 7 bar and room temperature. After
165 immobilization, the column was flushed with sodium borohydride (2.5 mg mL⁻¹, phosphate buffer 67
166 mM pH 8) (2 h, 7 bar) to reduce residual aldehydes. The Streptavidin columns were then rinsed with
167 phosphate buffer and stored at 4 °C.

168 2.4 Nano-FAC experiments

169 Nano-FAC Setup. Frontal Weak Affinity Chromatography experiments were carried out with a 7100
170 capillary electrophoresis Agilent system (Agilent Technologies, Waldbronn, Germany) equipped with
171 an external nitrogen tank to reach pressures up to 12bar. System control and data acquisition were
172 carried out using the Chemstation software (Agilent). All experiments were carried out in “short-end”
173 injection mode, with the inlet of the capillary immersed in the solution to be infused, so that by
174 applying external pressure at 12bar the liquid is forced to flow inside the capillary column. The
175 detection was achieved *in-situ* on an empty section of the column, right after the end of the monolith,
176 thanks to a diode array detector operated in multi-wavelength mode. [18] The revelation window on
177 the capillary was obtained by burning away the external coating of the capillary. The analyses were all
178 carried out under controlled room temperature at 25°C.

179 2.4.1 FAC for the evaluation of non-specific interactions

180 Non-specific interactions were evaluated by infusing compounds individually (100 μM solutions
181 prepared in phosphate buffer, 67 mM, pH=7,4) on the reduced aldehyde monolithic support until the
182 breakthrough time was reached. The columns were rinsed for 30 min in-between each infusion. The
183 breakthrough time is measured for each compound. In the case of non-specific interactions, this
184 breakthrough time $t_{\text{breakthrough}}$ is independent of the solute concentration [L] provided this

185 concentration is low enough to work is the linear range of the adsorption isotherm. If no non-specific
186 interactions take place, the breakthrough time occurs at the dead time (the reduced breakthrough
187 time is equal to 1). If non-specific interactions occur, the solute is captured by the support until the
188 equilibrium is reached, and the breakthrough time $t_{breakthrough}$ is delayed. The higher the non-specific
189 interactions, the higher the quantity of solute captured and the higher the breakthrough time.

$$190 \quad q_{capt} = (t_{breakthrough} - t_0) * F * [L] = \frac{(t_{breakthrough} - t_0)}{t_0} * V_0 * [L] = k_{ns} * V_0 * [L]$$

191 Where F is the flow rate, t_0 the dead time, V_0 the dead volume of the column and k_{ns} the retention
192 factor of the solute due to non-specific interactions.

193 2.4.2 Quantification of the number of protein active sites

194 For the determination of the amount of streptavidin active sites available after grafting, HABA ($K_d =$
195 $100 \mu\text{M}$) was infused as test solute with increasing concentrations (5, 10, 50, 100 and $200 \mu\text{M}$ solutions
196 prepared in phosphate buffer, 67 mM, $\text{pH}=7,4$), without any rinsing step in-between the percolation
197 of different concentrations (staircase experiments). The amount of ligand captured at each step is
198 determined and the cumulated amount of ligand captured is calculated by summing the captured
199 quantity at all the steps. The double reciprocal plot showing the amount of ligand captured vs the
200 ligand concentration allows for the simultaneous determination of both the K_d value of the
201 target–ligand interaction and the number of active sites available (Bact) (see S1 for the rationale of the
202 staircase approach). Rationality of the results was ensured by comparing the obtained K_d value (range
203 $90\text{-}120 \mu\text{M}$) with literature values ($100 \mu\text{M}$).

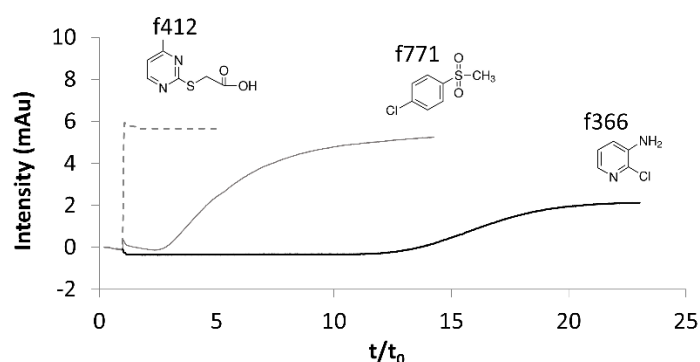
204

205 3- Results and discussion

206 3.1 Investigation of non-specific interactions on GMA-co-EDMA monoliths

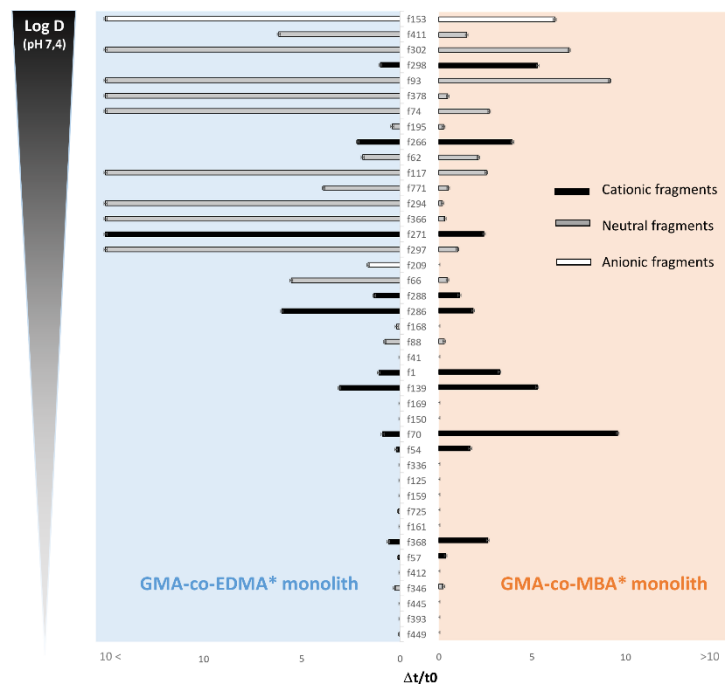
207 The starting monolith uses glycidyl methacrylate (GMA) as functional monomer and ethylene
208 dimethacrylate (EDMA) as crosslinker. Preparation of (bio)affinity monoliths requires their subsequent
209 functionalization with target (bio)molecules such as proteins. The preferred functionalization pathway
210 implements the hydrolysis of epoxides, followed by the periodate-mediated oxidation of the resulting
211 diols into aldehyde reactive groups. The protein is then covalently grafted onto the monolith via Schiff
212 base method. The remaining aldehyde groups after the grafting step are reduced to form alcohol
213 groups (Figure S2). This biofunctionalization method gives more hydrophilic stationary phases
214 compared to the one obtained by direct grafting of proteins onto the GMA-based monolith [7]. In
215 addition, the reaction is faster and results in improved grafting protein densities compared to the

216 epoxy method [20,21]. Using a 75- μm inner diameter capillary, up to 8 ± 0.3 pmol of active streptavidin
217 binding sites per cm of monolith are reached. The investigation of non-specific interactions on GMA-
218 co-EDMA based monoliths (interactions with the underlying material and not the whole affinity
219 column) was carried out on GMA-co-EDMA monoliths subjected to the entire functionalization process
220 except for the protein grafting step, viz on reduced aldehyde GMA-co-EDMA monoliths. Figure 1
221 presents the breakthrough curves obtained by nano-FAC experiments for three different molecules of
222 the library solubilized in a 67 mM phosphate buffer at pH=7,4. For f412, non-specific interactions are
223 not observed, and the breakthrough time is equal to the dead time ($k=0$). The presence of non-specific
224 interactions between the ligands and the stationary phase is observed by a shift of the breakthrough
225 curve from the dead time. The higher the non-specific interactions the higher the breakthrough times
226 as for f771 (a moderately retained compound, $k=3.9$) and f366 (a highly retained compound $k=14.7$)
227 (Figure 1).



228
229 Figure 1. Nano-FAC-UV chromatograms of three molecules exhibiting different retention behavior on
230 the reduced aldehyde GMA-co-EDMA monolith. Ligands were infused in pH 7.4 phosphate buffer
231 solution at 67 mM and detected at 230, 254 and 280 nm, respectively for f771, f412 and f366.

232
233 The retention factors (reduced breakthrough times) measured for the 41 molecules are ranked in
234 ascending order of their logarithm value of the distribution coefficient ($\log D$). All the experiments
235 were carried out in purely aqueous mobile phase at pH 7.4, i.e., in the experimental conditions
236 classically used for affinity studies. Results are summarized in Figure 2 (left).



237

238 Figure 2. Bar graphs of the reduced breakthrough times for the 41 molecules on reduced aldehyde
 239 GMA-co-EDMA* monolith (left) and reduced aldehyde GMA-co-MBA* monolith (right).

240

241 The ranking of the fragments according to their $\log D$ value (at pH 7.4) allows to feature the correlation
 242 between the retention and the hydrophobic character of test compounds, whatever the net charge of
 243 the molecules (Figure 2 left). Classification of the ligands according to other molecular or
 244 physicochemical properties (the whole molecular descriptors used are listed in table S1) did not reveal
 245 any other correlation. So, despite efforts to limit hydrophobicity of this monolithic stationary phase,
 246 non-specific interactions seem to be mainly governed by hydrophobic effects. Reducing these
 247 undesirable interactions involves increasing the hydrophilicity of the monolithic support. Two
 248 strategies have thus been considered: replacing the EDMA with a more hydrophilic crosslinker (MBA)
 249 and/or substituting part of the GMA functional monomer with a more hydrophilic monomer such as
 250 acrylamide [19] at the risk of reducing the amount of active epoxy groups *i.e.* the amount of protein
 251 that can be immobilized on the monolith.

252

253 3.2 Synthesis and characterization of GMA-co-MBA monoliths

254 Synthesis of GMA-co-MBA monoliths was carried out on the basis on the work of Zhu et al [19]. In this
 255 work, hydrophilic GMA-based monoliths were prepared using N, N' methylenebis(acrylamide) (MBA,
 256 $\log P$ -1.44) as crosslinker and acrylamide (AA, $\log P$ -0.77) as co- functional monomer with GMA ($\log P$

257 1.39). Although monolithic structures were easily obtained in our laboratory using the recipe proposed
258 by Zhu [19], the quantity of active proteins measured after grafting (less than 1 pmol cm^{-1}) was
259 significantly lower than on our GMA-co-EDMA monolith (to $8 \pm 0.3 \text{ pmol cm}^{-1}$). The optimization of the
260 monolith synthesis parameters (e.g., polymerization mixture composition, temperature and
261 polymerization time) was undergone to increase the density of active protein that can be grafted on
262 the monolithic stationary phase. Assuming the limiting factor is the density of glycidyl reactive groups
263 on the monolithic surface, the GMA/AA/MBA monomer ratio was modified, the porogen to monomer
264 ratio being kept constant (Table 1). GMA content was increased by decreasing acrylamide and MBA
265 content. The optimization criteria of the GMA-co-MBA monolith synthesis was based on the ability to
266 still obtain a monolith structure with a satisfactory permeability and on the quantity of active protein
267 that could be grafted. Best conditions of the thermally initiated polymerization (18 hours at $57 \text{ }^\circ\text{C}$)
268 gives rise to a quantity of immobilized active protein of $13 \pm 0.8 \text{ pmol per cm}$ of monolith. This is a big
269 improvement over the initial monolith described by Zhu [19] and the GMA-co-EDMA monolith (8 ± 0.3
270 pmol cm^{-1}).

271 **Table 1. Comparison of the monomer composition of the GMA-co-MBA polymerization mixture of the initial recipe and**
272 **after optimization in this work to increase the active protein density.**

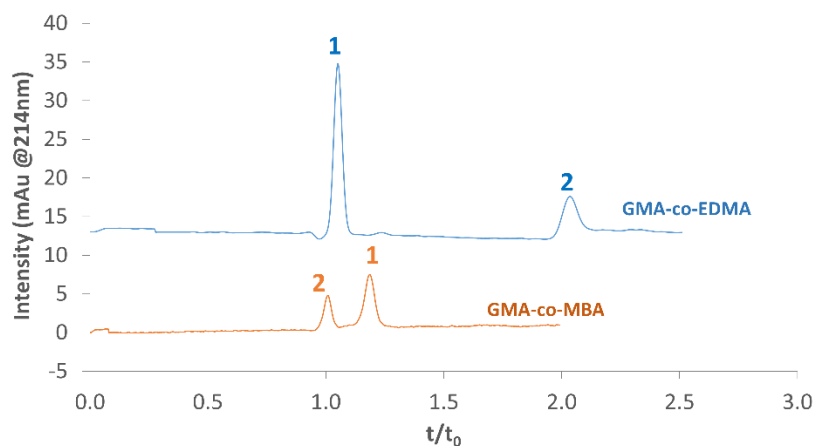
% monomer (w/w)	GMA-co-MBA [19]	GMA-co-MBA This work
GMA	24.8	60
Acrylamide	21.9	0
N,N'-methylenebis(acrylamide)	53.3	40

273

274 Although the protein content is a key parameter, our first goal was to increase the hydrophilicity of
275 the monolith. This was evaluated by following the retention behavior of two tests solutes (thiourea a
276 polar test solute with a log P value of -1.08 and octylbenzene a highly hydrophobic test solute with a
277 log P value of 6.6 in an acetonitrile /water (70:30, v:v) mobile phase. The two chromatograms are
278 illustrated Figure 3.

279

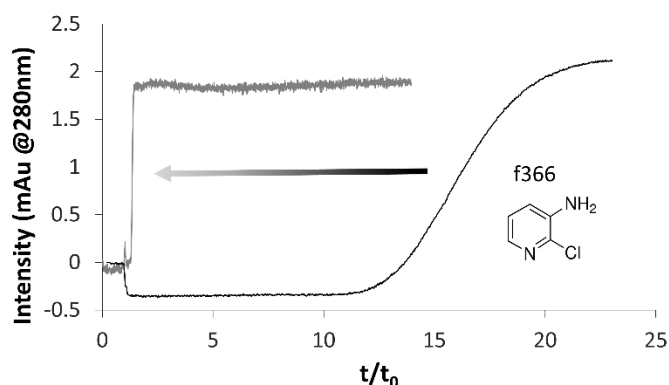
280



281
 282 Figure 3. Chromatograms of two test solutes on GMA-co-EDMA and GMA-co-MBA monoliths. Solutes :
 283 Injection of thiourea (1) and octylbenzene (2) in acetonitrile/water (70/30, v :v) mobile phase. UV
 284 detection at 254 nm. Applied pressure 12 bars.

285
 286 In these mobile phase conditions (acetonitrile /water, 70:30, v:v), the elution order of the two test
 287 solutes is reversed on the two monolithic columns. On the GMA-co-EDMA monolith, thiourea elutes
 288 at the hold-up time, while octylbenzene, which is more hydrophobic, elutes with a retention factor of
 289 approximately 1. This separation takes place according to a reversed-phase mechanism. On the GMA-
 290 co-MBA monolith and with the same mobile phase, the elution order is reversed, *viz* octylbenzene
 291 elutes first, indicative of a HILIC separation mechanism. Such a modification of the retention
 292 mechanism clearly reflects the highly hydrophilic character of this new GMA-co-MBA monolith
 293 stationary phase.

294 To investigate the benefits of this new monolith on non-specific interactions, the retention factors of
 295 the 41 fragment-like compounds were measured by nano-FAC on reduced aldehyde GMA-co-MBA
 296 monolith (GMA-co-MBA*) and compared with those obtained on reduced aldehyde GMA-co-EDMA
 297 monolith (GMA-co-EDMA*) (figure 2, right). As for the first study on GMA-co-EDMA monoliths all this
 298 set of experiments was carried out in a purely aqueous mobile phase buffered at pH=7.4. For most
 299 compounds, the non-specific interactions are drastically reduced. The higher the hydrophobic
 300 character of the solute, the higher the reduction of non-specific interactions. Figure 4 illustrates the
 301 impact of the reduction of the non-specific interaction for the ligand F366.



302

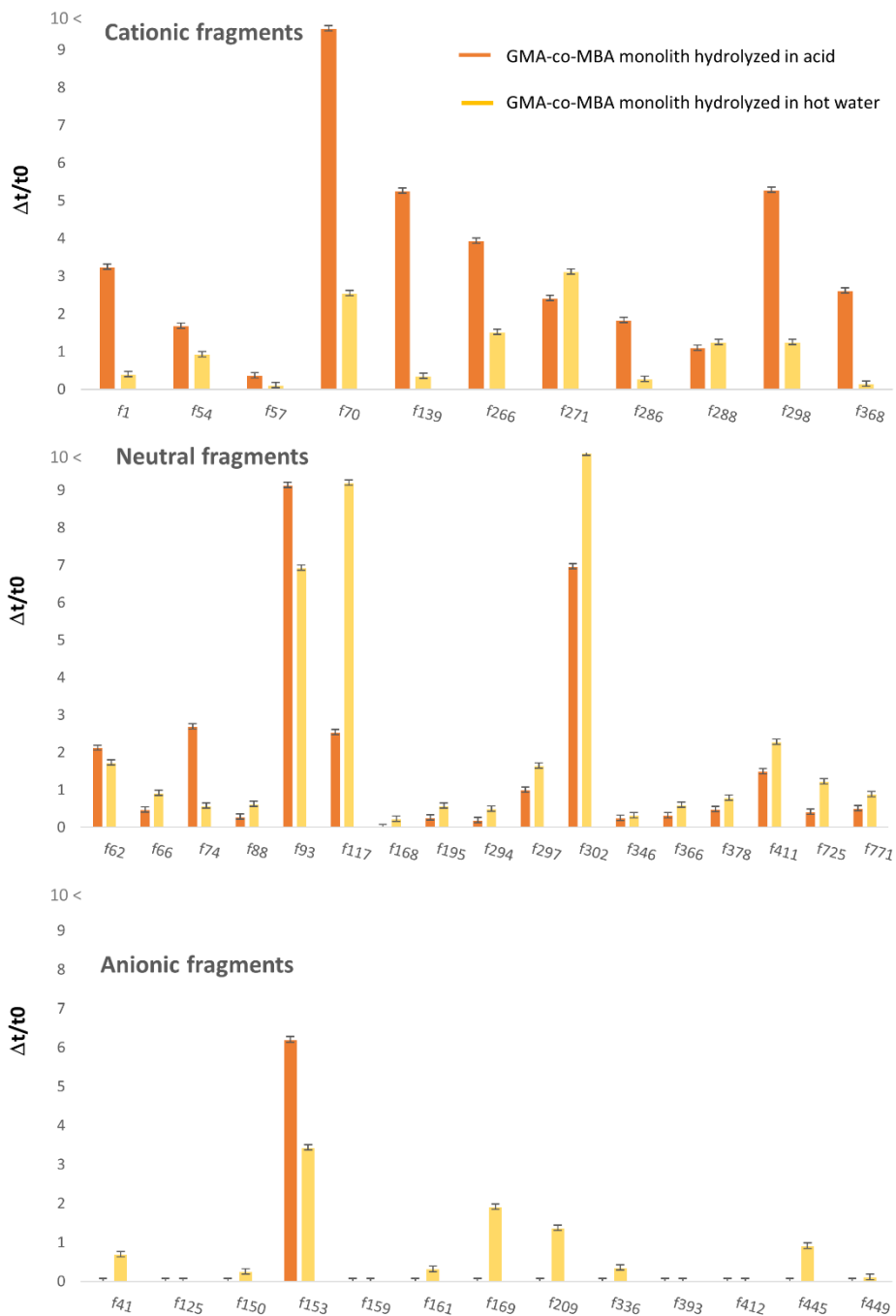
303 Figure 4. Nano-Frontal affinity chromatograms of the molecule F366 on the GMA-co-EDMA* and GMA-
 304 co-MBA* monolith. UV detection at 280 nm, mobile phase sodium acetate 20mM pH 7.4.

305

306 However, this effect observed for hydrophobic neutral compounds must be qualified by the increase
 307 in retention for some cationic compounds. This unexpected side effect on cationic compounds led us
 308 to seek its origin. A systematic investigation of the non-specific interactions observed for cationic
 309 compounds was performed at the different stages of functionalization. This non-specific interactions
 310 with cationic compounds appear from the first acid hydrolysis step. One hypothesis is the potential
 311 degradation of the acrylamide functions into carboxylic acids [22]. An alternative hydrolysis route to
 312 acid hydrolysis has therefore been evaluated to avoid this side-effect. A hot water hydrolysis step was
 313 therefore studied [23,24].

314 3.3 Optimization of the GMA-co-MBA monolith preparation: hot water hydrolysis

315 Following the reported procedures, GMA-co-MBA monolithic capillary columns were subjected to
 316 thermal treatment in hot water at 80°C for 18 h before undergoing the subsequent streptavidin
 317 grafting step. The efficiency of this hydrolysis of the epoxide groups method was evaluated through
 318 the determination of the quantity of grafted protein after the overall process. An amount of
 319 streptavidin binding sites of $16 \pm 0.8 \text{ pmol cm}^{-1}$ was obtained. While longer than acidic hydrolysis, this
 320 milder method using hot water is also effective to prepare affinity columns. To determine the impact
 321 of such modification on the physico-chemical properties of the resulting monolith, the retention
 322 behavior of the 41 ligands on reduced aldehyde GMA-co-MBA* monolith prepared by hot water
 323 hydrolysis was compared to those obtained by acidic hydrolysis. Figure 5 compares the reduced
 324 breakthrough times measured on the two GMA-co-MBA* monoliths. For clarity purpose, the ligands
 325 were classified by charge state (anionic, neutral and cationic ligands).



326

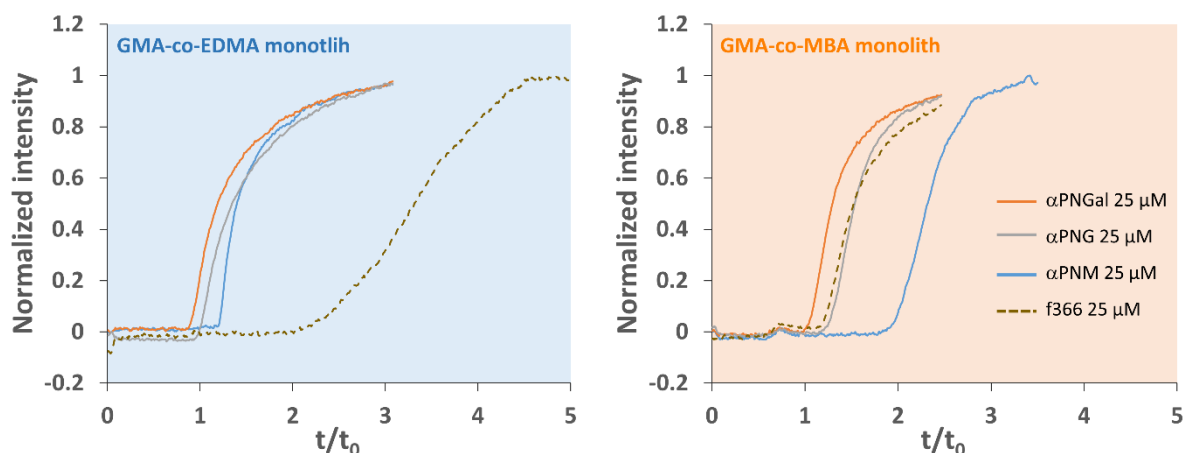
327 Figure 5. Bar graphs of the breakthrough times for the 41 molecules (classified according to their global
 328 charge: anionic, cationic or neutral fragments) on reduced aldehyde GMA-co-MBA* monolith
 329 hydrolyzed in acid (orange) and reduced aldehyde GMA-co-MBA* monolith hydrolyzed in hot water
 330 (yellow).

331 Regarding cationic fragments, except for compound f221 that is not affected, the hot water hydrolysis
332 drastically reduced the level of non-specific interactions observed by nano-FAC experiments.
333 Meanwhile, this new preparation method has not significantly modified the retention factor for neutral
334 ligands, except for f117 and f302 for unknown reason. On the contrary, the retention of anionic ligands
335 slightly increased. The very low level of retention of anionic ligands on the GMA-co-MBA* monolith
336 prepared by acid hydrolysis seems to be stressed by repulsive ionic interactions between species of
337 the same charge. Hydrolysis in hot water is intended to suppress the presence of anionic charge on the
338 support. In return, the level of retention of anionic ligands slightly increases. The modification of the
339 physico-chemical properties of the monolith generated by the modification of the mode of hydrolysis
340 seems to confirm the initial hypothesis according to which the high level of retention for the cationic
341 ligands came from the presence of negatively charged groups created during the acidic hydrolysis step.
342 In addition to graft as much as protein than with the previous one, this new hydrolysis method
343 drastically reduced the level of non-specific interactions for the cationic ligands without affecting the
344 non-specific interactions for the neutral and anionic ligands. The stability of this GMA-co-MBA
345 monolith hydrolyzed in hot water was evaluated. The retention factors remained constant for the
346 duration of use (one week of continuous use) and even after 3 additional months of storage (the
347 column was store in aqueous solution at room temperature).

348 3.4 Application of the new GMA-co-MBA monolithic affinity columns for the measurement of protein 349 (Con A)-ligand interactions

350 Use of FAC for ligand screening generally relies on the comparison of breakthrough curves of a set of
351 compounds using a protein immobilized on the stationary phase. Working at a fixed ligand
352 concentration, the longer the breakthrough time, the higher the affinity. This straightforward
353 relationship turns out to be more complex when non-specific interactions are not negligible. It is
354 therefore necessary to find methodological strategies to avoid misinterpretation. For example, it is
355 possible to use control columns without protein to assess the retention level due to non-specific
356 interactions on the stationary phase itself. Minimizing the non-specific interactions is necessary both
357 for reducing the duration of experiments and limiting false positives. To illustrate the impact of non-
358 specific interactions during screening experiments and show the improvement in the use of a
359 stationary phase that limits non-specific contributions, nano-FAC experiments were performed on
360 GMA-co-EDMA and GMA-co-MBA monoliths. Concanavalin A, a lectin that binds mannose-containing
361 ligands with high affinity, or other carbohydrates with lower affinities [25–27], was used as protein
362 model. Four ligands were used to illustrate the impact of the non-specific interactions when screening
363 ligand by nano-FAC. P-nitro- α -D-mannopyranoside (α PNM) and P-nitro- α -D-glucopyranoside (α PNG)

364 were used as low affinity ligands (Kd values of 50 μ M and > 200 μ M, respectively [27]) and P-nitro- α -
365 D-galactopyranoside (α PNGal) and f366 were used as controls (non-ligands).



366

367 Figure 6. Nano-Frontal affinity chromatograms of α PNM, α PNG, α PNGal and the molecule f366 on the
368 GMA-co-EDMA and GMA-co-MBA monolith. UV detection at 240 nm for the molecule f366 and 300
369 nm for α PNM, α PNG and α PNGal. Mobile phase sodium acetate 20mM pH 7.4.

370

371 Figure 6 shows the frontal affinity chromatograms obtained for the 4 tested ligands on both stationary
372 phases. Regarding the glycosides residues, the galactose residue (α PNGal as a non-ligand of ConA
373 elutes early followed by α PNG and α PNM) on the two columns. These stereoisomers of monoglycoside
374 share comparable physico-chemical properties and are highly polar compounds. This supports the
375 observed behavior of α PNGal that elutes at the hold-up time of the column ($t/t_0=1$). The order of
376 elution follows the affinity of the three ligands. The situation is more complex if we look to the more
377 hydrophobic ligand f366. On the GMA-co-EDMA column, this ligand elutes in last position while it
378 elutes with α PNGal on the MBA-co-EDMA column. F366 is a neutral and moderately nonpolar
379 compound ($\log D = 0.97$ at pH 7.4). Interpretation of the raw breakthrough curves on the GMA-co-
380 EDMA monolith would lead to a wrong conclusion about the affinity of the ligands for f366. Conversely,
381 the use of the highly polar GMA-co-MBA column allows to conserve the order of elution logical with
382 respect to the ligand affinity. Moreover, the higher amount of active ConA grafted on the monolith
383 allows a better discrimination between solutes with different Kd values.

384

385 4- Conclusions

386 In affinity chromatography, non-specific interactions between the ligands and the chromatographic
387 support may affect the results, leading to misinterpretations during the investigation of protein-ligand
388 interactions (detection of false positives in ligand screening, lack of specificity in purification).
389 Optimizing the underlying support of the affinity column to reduce nonspecific interactions is an
390 ongoing goal. A new methodology was first proposed for the characterization of non-specific
391 interactions. This methodology relies on the determination of the retention behavior of a set of 41
392 selected small molecules. Such methodology applied to GMA-co-EDMA monolithic capillary columns
393 has shown that non-specific interactions are mainly due to hydrophobic effects and must be taken into
394 account. This led us to propose the modification of the monolith synthesis by using MBA crosslinker to
395 increase the hydrophilicity of the resulting monolith. A large reduction of non-specific interactions was
396 observed for all the ligands excepted the cationic ones. This behavior of cationic solutes has been
397 attributed to electrostatic interactions with the monolith after the acidic hydrolysis step (side reaction
398 onto the MBA crosslinker). Acidic hydrolysis was successfully replaced by a hot water treatment. The
399 new poly(GMA-co-MBA) monolith not only exhibits improved hydrophilic surface properties, but also
400 higher protein density (16 ± 0.8 pmol cm^{-1} instead of 8 ± 0.3 pmol cm^{-1} for the GMA-co-EDMA monolith).
401 The new highly hydrophilic monolith should find applications in various fields of affinity
402 chromatography (e.g., sample purification, preconcentration, chiral separation, IMERs ...).

403

404 Acknowledgements

405 The author(s) acknowledge(s) the support of the French Agence Nationale de la Recherche (ANR),
406 under grant ANR-21-CE29-0012 (project NanoWAC).

407 References

- 408 [1] Z. Li, E. Rodriguez, S. Azaria, A. Pekarek, D.S. Hage, Affinity monolith chromatography: A review
409 of general principles and applications, *ELECTROPHORESIS*. 38 (2017) 2837–2850.
410 <https://doi.org/10.1002/elps.201700101>.
- 411 [2] E. Calleri, S. Ambrosini, C. Temporini, G. Massolini, New monolithic chromatographic supports
412 for macromolecules immobilization: Challenges and opportunities, *Rev. Pap. Pharm. Biomed. Anal.*
413 2012. 69 (2012) 64–76. <https://doi.org/10.1016/j.jpba.2012.01.032>.
- 414 [3] E.L. Pfaunmiller, M.L. Paulemond, C.M. Dupper, D.S. Hage, Affinity monolith chromatography: a
415 review of principles and recent analytical applications, *Anal. Bioanal. Chem.* 405 (2013) 2133–2145.
416 <https://doi.org/10.1007/s00216-012-6568-4>.
- 417 [4] H.M. Almughamsi, M.K. Howell, S.R. Parry, J.E. Esene, J.B. Nielsen, G.P. Nordin, A.T. Woolley,
418 Immunoaffinity monoliths for multiplexed extraction of preterm birth biomarkers from human blood

419 serum in 3D printed microfluidic devices, *Analyst*. 147 (2022) 734–743.
420 <https://doi.org/10.1039/D1AN01365C>.

421 [5] S. Jiang, Z. Zhang, L. Li, A one-step preparation method of monolithic enzyme reactor for highly
422 efficient sample preparation coupled to mass spectrometry-based proteomics studies, *J Chromatogr*
423 *A*. 1412 (2015) 75–81. <https://doi.org/10.1016/j.chroma.2015.07.121>.

424 [6] J. Guo, Q. Wang, D. Xu, J. Crommen, Z. Jiang, Recent advances in preparation and applications of
425 monolithic chiral stationary phases, *TrAC Trends Anal. Chem.* 123 (2020) 115774.
426 <https://doi.org/10.1016/j.trac.2019.115774>.

427 [7] L. Lecas, J. Randon, A. Berthod, V. Dugas, C. Demesmay, Monolith weak affinity chromatography
428 for μg -protein-ligand interaction study, *J. Pharm. Biomed. Anal.* 166 (2019) 164–173.
429 <https://doi.org/10.1016/j.jpba.2019.01.012>.

430 [8] L. Lecas, L. Hartmann, L. Caro, S. Mohamed-Bouteben, C. Raingeval, I. Krimm, R. Wagner, V.
431 Dugas, C. Demesmay, Miniaturized weak affinity chromatography for ligand identification of
432 nanodiscs-embedded G-protein coupled receptors, *Anal. Chim. Acta.* 1113 (2020) 26–35.
433 <https://doi.org/10.1016/j.aca.2020.03.062>.

434 [9] D.N. Gunasena, Z. El Rassi, Hydrophilic diol monolith for the preparation of immuno-sorbents at
435 reduced nonspecific interactions, *J. Sep. Sci.* 34 (2011) 2097–2105.
436 <https://doi.org/10.1002/jssc.201100353>.

437 [10] S. Khadka, Z. El Rassi, Postpolymerization modification of a hydroxy monolith precursor. Part III.
438 Activation of poly(hydroxyethyl methacrylate-co-pentaerythritol triacrylate) monolith with epoxy
439 functionalities followed by bonding of glycerol, polyamines, and hydroxypropyl- β -cyclodextrin for
440 hydrophilic interaction and chiral capillary electrochromatography, *ELECTROPHORESIS*. 37 (2016)
441 3178–3185. <https://doi.org/10.1002/elps.201600326>.

442 [11] F. Svec, Porous polymer monoliths: Amazingly wide variety of techniques enabling their
443 preparation, *Ed. Choice IV*. 1217 (2010) 902–924. <https://doi.org/10.1016/j.chroma.2009.09.073>.

444 [12] M. Vergara-Barberán, E.J. Carrasco-Correa, M.J. Lerma-García, E.F. Simó-Alfonso, J.M. Herrero-
445 Martínez, Current trends in affinity-based monoliths in microextraction approaches: A review, *Anal.*
446 *Chim. Acta.* 1084 (2019) 1–20. <https://doi.org/10.1016/j.aca.2019.07.020>.

447 [13] M.B. Espina-Benitez, J. Randon, C. Demesmay, V. Dugas, Development and application of a new
448 in-line coupling of a miniaturized boronate affinity monolithic column with capillary zone
449 electrophoresis for the selective enrichment and analysis of cis-diol-containing compounds, *J.*
450 *Chromatogr. A*. 1494 (2017) 65–76. <https://doi.org/10.1016/j.chroma.2017.03.014>.

451 [14] M.B. Espina-Benitez, F. Marconi, J. Randon, C. Demesmay, V. Dugas, Evaluation of boronate
452 affinity solid-phase extraction coupled in-line to capillary isoelectric focusing for the analysis of

453 catecholamines in urine, *Anal. Chim. Acta.* 1034 (2018) 195–203.
454 <https://doi.org/10.1016/j.aca.2018.06.017>.

455 [15] J.C. Masini, F. Svec, Porous monoliths for on-line sample preparation: A review, *Anal. Chim. Acta.*
456 964 (2017) 24–44. <https://doi.org/10.1016/j.aca.2017.02.002>.

457 [16] M. Nechvátalová, J. Urban, Current trends in the development of polymer-based monolithic
458 stationary phases, *Anal. Sci. Adv.* 3 (2022) 154–164. <https://doi.org/10.1002/ansa.202100065>.

459 [17] S. Poddar, S. Sharmeen, D.S. Hage, Affinity monolith chromatography: A review of general
460 principles and recent developments, *ELECTROPHORESIS.* 42 (2021) 2577–2598.
461 <https://doi.org/10.1002/elps.202100163>.

462 [18] A. Gottardini, C. Netter, V. Dugas, C. Demesmay, Two Original Experimental Setups for
463 Staircase Frontal Affinity Chromatography at the Miniaturized Scale, *Anal. Chem.* 93 (2021) 16981–
464 16986. <https://doi.org/10.1021/acs.analchem.1c04772>.

465 [19] G. Zhu, H. Yuan, P. Zhao, L. Zhang, Z. Liang, W. Zhang, Y. Zhang, Macroporous polyacrylamide-
466 based monolithic column with immobilized pH gradient for protein analysis, *ELECTROPHORESIS.* 27
467 (2006) 3578–3583. <https://doi.org/10.1002/elps.200600189>.

468 [20] R. Mallik, D.S. Hage, Affinity monolith chromatography, *J. Sep. Sci.* 29 (2006) 1686–1704.
469 <https://doi.org/10.1002/jssc.200600152>.

470 [21] T. Jiang, R. Mallik, D.S. Hage, Affinity Monoliths for Ultrafast Immunoextraction, *Anal. Chem.* 77
471 (2005) 2362–2372. <https://doi.org/10.1021/ac0483668>.

472 [22] Y. Pei, L. Zhao, G. Du, N. Li, K. Xu, H. Yang, Investigation of the degradation and stability of
473 acrylamide-based polymers in acid solution: Functional monomer modified polyacrylamide,
474 *Petroleum.* 2 (2016) 399–407. <https://doi.org/10.1016/j.petlm.2016.08.006>.

475 [23] Z. Wang, Y.-T. Cui, Z.-B. Xu, J. Qu, Hot Water-Promoted Ring-Opening of Epoxides and Aziridines
476 by Water and Other Nucleophiles, *J. Org. Chem.* 73 (2008) 2270–2274.
477 <https://doi.org/10.1021/jo702401t>.

478 [24] L.P.D. Ratcliffe, A.J. Ryan, S.P. Armes, From a Water-Immiscible Monomer to Block Copolymer
479 Nano-Objects via a One-Pot RAFT Aqueous Dispersion Polymerization Formulation, *Macromolecules.*
480 46 (2013) 769–777. <https://doi.org/10.1021/ma301909w>.

481 [25] K. KASAI, Frontal affinity chromatography: A unique research tool for biospecific interaction that
482 promotes glycobiology, *Proc. Jpn. Acad. Ser. B Phys. Biol. Sci.* 90 (2014) 215–234.
483 <https://doi.org/10.2183/pjab.90.215>.

484 [26] K. Kasai, Frontal affinity chromatography: An excellent method of analyzing weak biomolecular
485 interactions based on a unique principle, *Biochim. Biophys. Acta BBA - Gen. Subj.* 1865 (2021) 129761.
486 <https://doi.org/10.1016/j.bbagen.2020.129761>.

487 [27] Y. Oda, K. Kasai, S. Ishii, Studies on the Specific Interaction of Concanavalin A and Saccharides by
488 Affinity Chromatography. Application of Quantitative Affinity Chromatography to a Multivalent
489 System, J. Biochem. (Tokyo). 89 (1981) 285–296.
490 <https://doi.org/10.1093/oxfordjournals.jbchem.a133192>.
491